

EG1100478

Study the Validity of the Direct Mathematical Method for Calculation the Total Efficiency Using Point and Disk Sources

Mohamed A. Naeem², Ahmed M. El Khatib², Ossama M. Hagag¹, Shereif S. Nafee²

¹Physics Department, Faculty of Science, Port Said University, Alexandria, Egypt.

²Physics Department, Faculty of Science, Alexandria University, Alexandria, Egypt.

E-mail : hagag82@yahoo.com

ABSTRACT

The direct mathematical method has been developed for calculating the total efficiency of many cylindrical gamma detectors, especially HPGe & NaI detector. Different source geometries are considered (point & disk). Further into account is taken of gamma attenuation from detector window or any interfacing absorbing layer. Results are compared with published experimental data to study the validity of the direct mathematical method to calculate total efficiency for any gamma detector size.

Keywords: *Mathematical methods / Cylindrical gamma detector / Total efficiency.*

INTRODUCTION

In gamma ray spectrometry the total efficiency is defined as “the ratio between the number of photons that are recorded in the detector with any possible energy during a certain time interval and the number of photons that are emitted by the source during the same time interval”. Several authors [1-11] have treated the total efficiency and have given useful solutions. This paper describes direct mathematical method (proved by Selim and Abbas [12-18] to calculate the total efficiency for a cylindrical gamma detector for an axial point and thin coaxial circular disk sources emitting photons with wide energy range located at different heights from the detector surface.

The mathematical integrals used for calculating the efficiency of an axial point and thin coaxial circular disk sources with a cylindrical detector are evaluated numerically. Section 2 presents direct mathematical formulae for the total efficiency in three different cases (axial point, non axial point and extended thin coaxial circular disk sources).

The attenuation of photons by the detector end cap materials or any absorber also presented in simple straightforward mathematical expressions. Section 3 contains comparisons between the calculated total efficiency using the formulae derived in this work with the published experimental data to study the validity of the present mathematical formulae. Conclusions are presented in section 4.

2) MATHEMATICAL VIEWPOINT

By using spherical coordinate, the integration limits change in steps in accordance to the values of the effective traversed distance d and the polar angle θ and φ . The geometry of coaxial point source to the cylindrical detector ($2R \times L$) is given in (Fig 1). Where ρ is point source displaced distance from the detector's axis.

The general equation for the detector efficiency for an isotropic radiating point source can be expressed by [2]:

$$\varepsilon_{\text{point}} = \frac{1}{4\pi} \int_{\theta} \int_{\varphi} f_{\text{att}} (1 - e^{-\mu \cdot d}) \sin\theta \, d\varphi \, d\theta \quad (1)$$

Considering the symmetry around the azimuth angle, φ , equation (1) can be written as [3]:

$$\varepsilon_{\text{point}} = \frac{1}{4\pi} \sum_{i=1}^n Y_i \quad (2)$$

Where:

$$\left. \begin{aligned} Y_i &= \int_{\theta} \int_{\varphi} f_{\text{att}} \cdot f_i \sin\theta \, d\varphi \, d\theta \\ f_i &= (1 - e^{-\mu \cdot d_i}) \end{aligned} \right\} \quad (3)$$

Where, d_i , are the possible path lengths traveled by the photon within the detector active volume depending on the position of incidence photon, d_1, d_2, \dots, d_n , as will be discussed later, and the attenuation, f_{att} , for absorber layers, $\mu_1, \mu_2, \dots, \mu_n$, with thickness, t_1, t_2, \dots, t_n , between the source and front of the detector given by:

$$f_{\text{att}} = e^{-\sum_{i=1}^n \mu_i \delta_i} \quad \text{where, } \delta_i = \left(\frac{t_i}{\cos\theta} \right) \quad (4)$$

2.1) THE SOURCE IS AXIAL POINT SOURCE ($\rho=0$)

The distances covered by the photon in both cases are given by:

$$\left. \begin{aligned} d_1 &= \frac{L}{\cos\theta} \\ d_2 &= \frac{R}{\sin\theta} - \frac{h}{\cos\theta} \end{aligned} \right\} \quad (5)$$

Where, $(\theta_1 \text{ to } \theta_2)$ are the extreme values of the polar angles based on the source-detector configuration, and given by:

$$\left. \begin{aligned} \theta_1 &= \tan^{-1}\left(\frac{R}{h+L}\right) \\ \theta_2 &= \tan^{-1}\left(\frac{R}{h}\right) \end{aligned} \right\} \quad (6)$$

Therefore recalling equation (2) the efficiency is given by:

$$\varepsilon_{\text{point}} = \frac{1}{2\pi} \sum_{i=1}^{n=2} Y_i \quad (7)$$

Where:

$$Y_1 = \int_0^{\theta_1} \int_0^{\pi} f_{\text{att}} \cdot f_1 \sin \theta d\varphi d\theta \quad , \quad Y_2 = \int_{\theta_1}^{\theta_2} \int_0^{\pi} f_{\text{att}} \cdot f_2 \sin \theta d\varphi d\theta \quad (8)$$

2.2) NON-AXIAL POINT SOURCE AT A POSITION ($\rho < R$)

The distances traveled by the photon in both cases are given by:

$$\left. \begin{aligned} d_1 &= \frac{L}{\cos \theta} \\ d_2 &= \frac{\rho \cos \varphi + \sqrt{R^2 - \rho^2 \sin^2 \varphi}}{\sin \theta} - \frac{h}{\cos \theta} \end{aligned} \right\} \quad (9)$$

Where, (θ_1 to θ_4), are the extreme values of the polar angles based on the source-detector configuration, and given by:

$$\left. \begin{aligned} \theta_1 &= \tan^{-1}\left(\frac{R-\rho}{h+L}\right) \\ \theta_2 &= \tan^{-1}\left(\frac{R-\rho}{h}\right) \\ \theta_3 &= \tan^{-1}\left(\frac{R+\rho}{h+L}\right) \\ \theta_4 &= \tan^{-1}\left(\frac{R+\rho}{h}\right) \end{aligned} \right\} \quad (10)$$

The maximum azimuthal angles for the photon to enter from the upper face, φ_{max} , and to emerge from the bottom of the detector, φ'_{max} , are given by:

$$\left. \begin{aligned} \varphi_{\text{max}} &= \cos^{-1}\left(\frac{\rho^2 - R^2 + h^2 \tan^2 \theta}{2\rho h \tan \theta}\right) \\ \varphi'_{\text{max}} &= \cos^{-1}\left(\frac{\rho^2 - R^2 + (h+L)^2 \tan^2 \theta}{2\rho(h+L)\tan \theta}\right) \end{aligned} \right\} \quad (11)$$

There are two cases according to the values of the polar angle, θ_i , ($\theta_1 < \theta_2 \leq \theta_3 < \theta_4$) and ($\theta_1 < \theta_3 < \theta_2 < \theta_4$). The efficiency can be given by:

$$\epsilon_{\text{point}} = \frac{1}{2\pi} \sum_{i=1}^{n=4} Y_i \quad (12)$$

Where:

$$\begin{aligned} Y_1 &= \int_0^{\theta_1} \int_0^{\pi} f_{\text{att}} \cdot f_1 \sin \theta d\phi d\theta, & Y_2 &= \int_{\theta_1}^{\theta_2} \int_0^{\pi} f_{\text{att}} \cdot f_2 \sin \theta d\phi d\theta \\ Y_3 &= \int_{\theta_1}^{\theta_3} \int_0^{\phi_{\text{max}}} f_{\text{att}} \cdot f_1 \sin \theta d\phi d\theta - \int_{\theta_1}^{\theta_3} \int_0^{\phi_{\text{max}}} f_{\text{att}} \cdot f_2 \sin \theta d\phi d\theta \\ Y_4 &= \int_{\theta_2}^{\theta_4} \int_0^{\phi_{\text{max}}} f_{\text{att}} \cdot f_2 \sin \theta d\phi d\theta \end{aligned} \quad (13)$$

2.3) THE CASE OF A THIN COAXIAL CIRCULAR DISK SOURCE

The detector efficiency in case of a disk source with radius, S, smaller than that, R, of the detector, (i.e., $S < R$), given as:

$$\epsilon_{\text{Disk}} = \frac{1}{\pi S^2} \int_0^{2\pi} \int_0^S \epsilon_{\text{point}}(\rho < R) \rho d\rho d\phi \quad (14)$$

VALIDATION OF THE PRESENT METHOD

We calculated the total efficiency for several cylindrical gamma detectors by using an axial point and thin coaxial circular disk sources emitting photons with wide range of energy located at different height from the detector surface.

The source-detector geometrical parameters and the source energy range plus the detector end cap type and thickness for all detectors are given in [Table 1], the comparison between the calculated values of the total efficiencies obtain by the present direct mathematical method with previous treatments (published data [19-21]) appear in Figure [4-7].

CONCLUSION

Direct mathematical expressions to calculate the total efficiency of cylindrical gamma detectors have been derived in the case of an axial point, non axial point and extended circular disk sources. From the comparison of the calculated values for the total efficiency with the published data, a good agreement has been achieved.

Figure captions

Figure 1: Axial point source with cylindrical detector ($\rho=0$).

Figure 2: Shows the possible cases of the photon path lengths through the detector active volume in case of ($\rho < R$).

Figure 3: Coaxial isotropically radiating circular disk source of radius S ($S \leq R$).

Figure 4: The variation of the total efficiency of an HPGe detector for a point source placed at the detector end cap (Detector 1 in Table 1).

Figure 5: Variation of total efficiency with the photon energy for the detector size (Detector 2 in Table 1).

Figure 6: Variation of total efficiency with the photon energy for the detector size (Detector 3 in Table 1).

Figure 7: Total efficiency for a NaI(Tl) detector with a disc source (Detector 4 in Table 1).

Table 1: The characteristics of source-detector geometrical arrangement

REFERENCES

- (1) Moens, L. and Hoste, J., Int. J. Appl. Radiat. Isot. 34, 1085 (1983).
- (2) Lippert, J., Int. J. Appl. Radiat. Isot. 34, 1097 (1983)
- (3) Wang, T.K., Mar, W.Y., Ying, T.H., Liao, C.H. and Tseng, C.L., Int. J. Appl. Radiat. Isot. 46, 933 (1995).
- (4) M.Y., Int. J. Appl. Radiat. Isot. 48, 83 (1997).
- (5) Wainio, K.M. and Knoll, G.F., Nucl. Instr. and Meth. 44, 213 (1996).
- (6) Nakamura, T., Nucl. Instr. and Meth. 205, 211 (1983).
- (7) Herold, L.K. and Kouzes, R.T., IEEE Trans. Nucl. Sci. NS-38, 231(1991).
- (8) Komboj, S. and Kahn, B., Health Phys. , 70, 512 (1996).
- (9) Jiang, S.H., Liang, J.H., Chou, J.T., Lin, U.T. and Yeh, w.w., Nucl. Instr. and Meth. A413, 281 (1998).
- (10) Selim, Y.S. and Abbas, M.I., Egypt. J. Phys. 26,(1/2): 79 (1995).
- (11) Selim, Y.S., Abbas, M.I. and Fawzy, M.A., Radiat, Phys. Chem. 53, 589 (1998).
- (12) Abbas, M.I., Radiat. Phys. Chem. 60, 3 (2001).
- (13) Abbas, M.I., Int. J. Appl. Radiat. Isot. 54, 761 (2001).
- (14) Abbas, M.I., Int. J. Appl. Radiat. Isot. 55, 245 (2001).
- (15) Abbas, M.I., Egypt. J. Phys. 32, 19 (2001).
- (16) Abbas, M.I. and Selim, Y.S., Nucl. Instr. and Meth. A480/2-3, 649 (2002).
- (17) Keyser, R.M., Twomey, T.R., Sangsingkeow, P., Journal of Radio analytical and Nuclear Chemistry, Vol. 244, No.3, 641-647 (2000).
- (18) Ronald Keyser, Timothy Twomey, Daniel Upp.
http://www.ortec-online.com/papers/inmm_2003_keyser.pdf
- (19) Abbas, M.I., Int. J. Appl. Radiat. Isot. 64, 1057-1064 (2006).
- (20) Gerhard Haase, David Tait , Arnold Wiechen. Nucl. Instrum. Methods A329 (1993)483-492.
- (21) S. Yalcina , Int. J. Appl. Radiat. Isot. 65, 1179-1186 (2007).

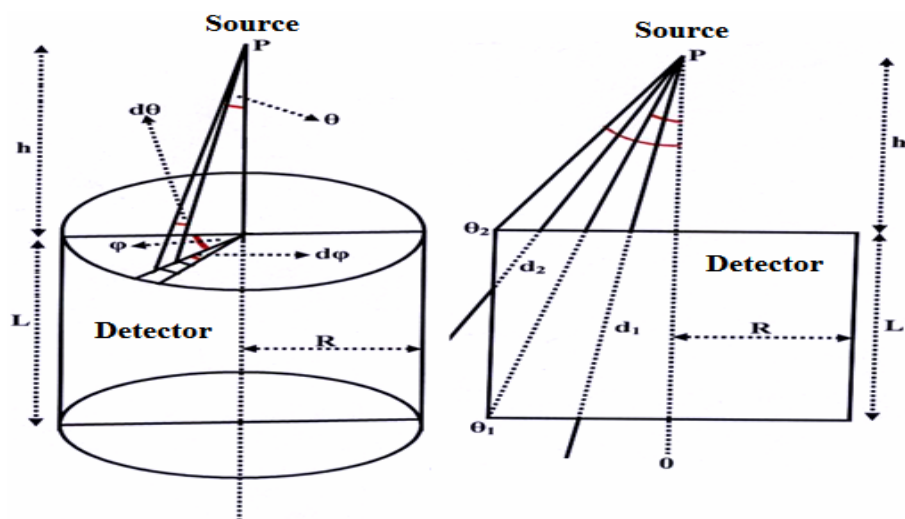


Figure 1

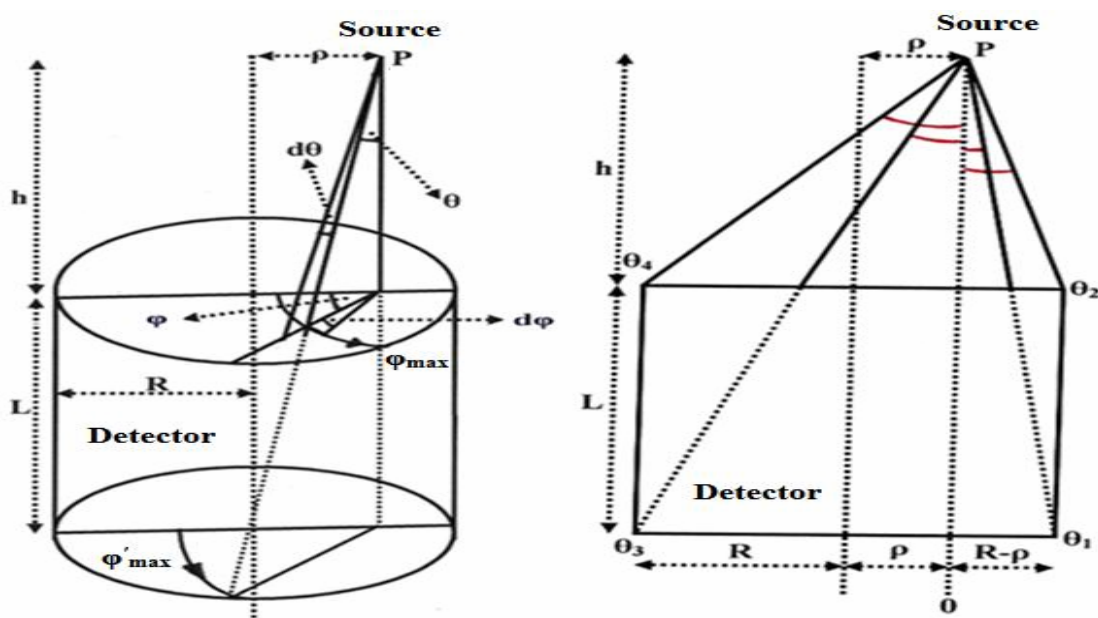


Figure 2

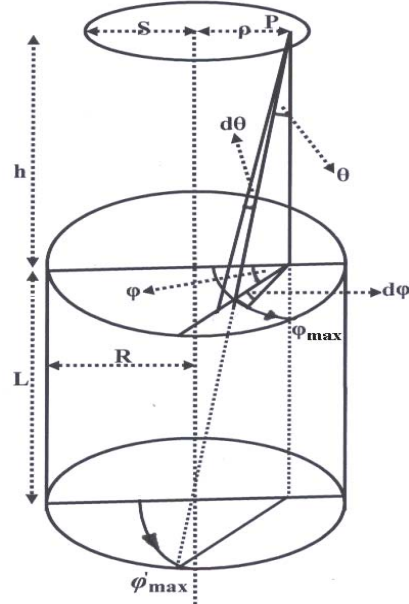


Figure 3

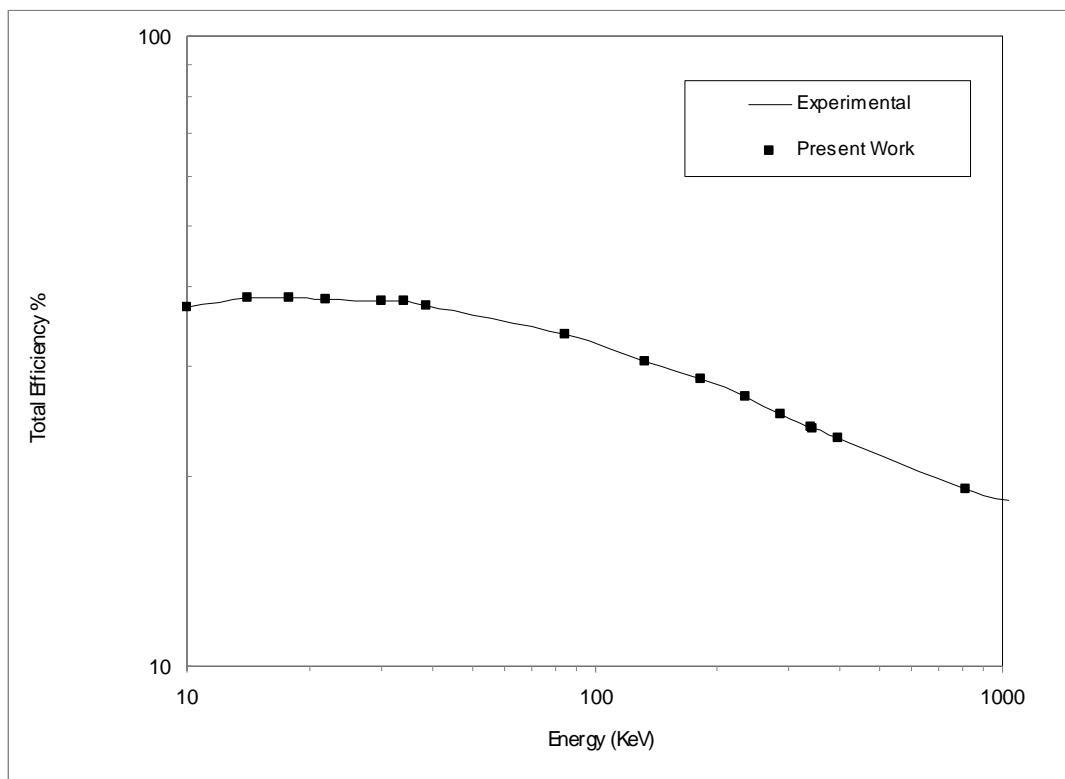


Figure 4

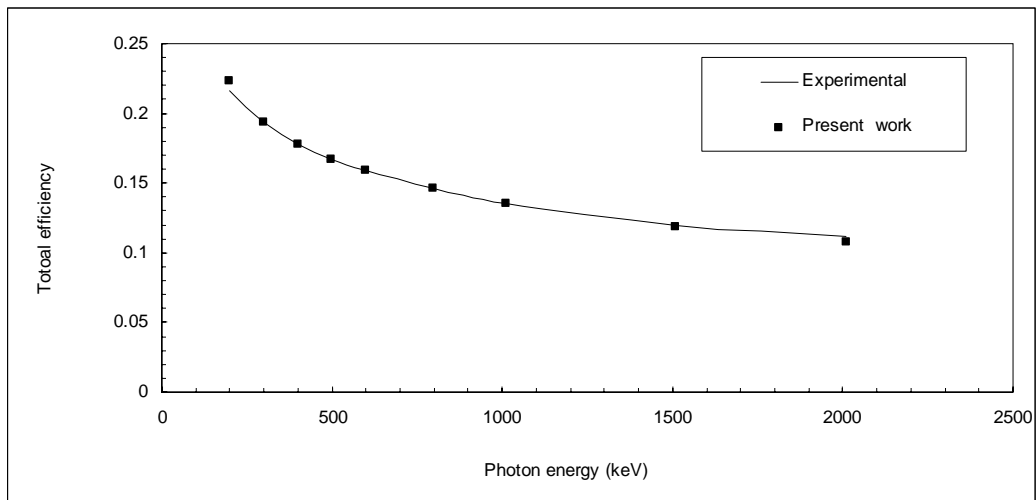


Figure 5

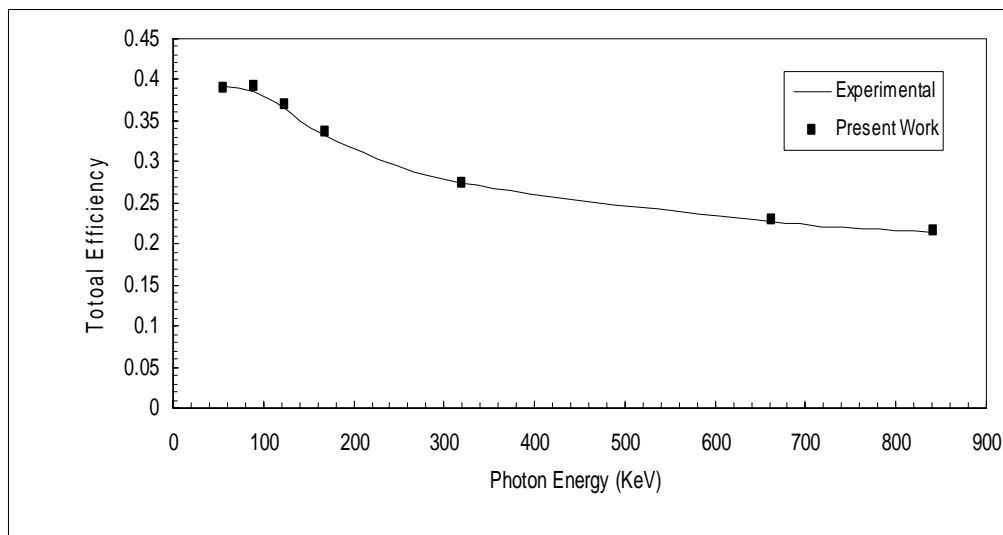


Figure 6

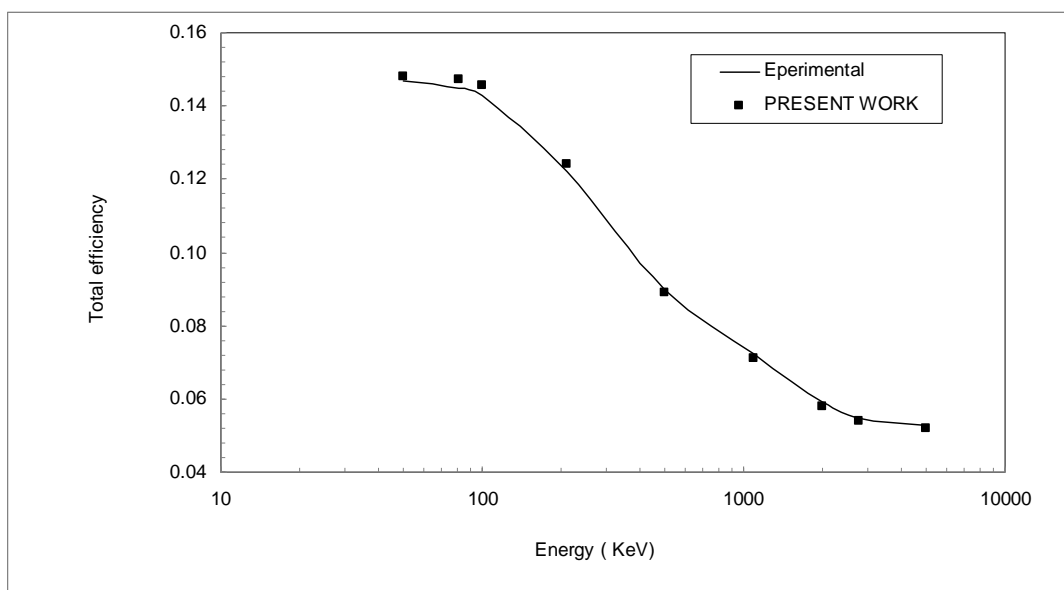


Figure 7

Table 1

Source-detector geometrical	Detector 1 HPGe	Detector 2 Ge(i)	Detector 3 HPGe	Detector 4 NaI(Tl)
Crystal radius	2.94 cm	2.15 cm	2.54 cm	7.62 cm
Crystal length	6.92 cm	4.65 cm	6.5 cm	3.81 cm
Detector end cap type and thickness	(Be) 0.05 cm	-	(Be)0.05 cm	-
Distance of source from the end cap	-	0.8	-	-
Distance between end cap and detector surface	0.5 cm	-	0.5 cm	3.0 cm
Source type	Point source	Point source	Point source	Disk source S = 3.81 cm